Postprint of: Nosko O., Jeffreys heat conduction in coupled semispaces subjected to interfacial heating, International Journal of Heat and Mass Transfer, Vol. 203 (2023), 123829, DOI: 10.1016/j.ijheatmasstransfer.2022.123829

Jeffreys heat conduction in coupled semispaces subjected to interfacial heating

Oleksii Nosko

Gdansk University of Technology, Faculty of Mechanical Engineering and Ship Technology,
ul. G. Narutowicza 11/12, Gdansk 80-233, Poland
E-mail: oleksii.nosko@pg.edu.pl

Keywords: Jeffreys heat conduction; Cattaneo heat conduction; hyperbolic heat conduction; perfect thermal contact; interfacial heat source; heat partition coefficient

A Jeffreys heat conduction problem for coupled semispaces subjected to the action of an interfacial heat source was defined. An analytical solution of the problem was derived for a polynomial specific power of the heat source using the Laplace transform approach. The asymptotic and parametric analysis was performed for different ratios of thermal conductivities $K_{1,2}$, thermal diffusivities $k_{1,2}$, thermal relaxation times $\tau_{1,2}$ and coefficients $\alpha_{1,2}$ indicating the relative contribution of Fourier heat conduction. It was found that Jeffreys heat conduction results in continuous variation of the contact temperature, whilst its particular case — Cattaneo heat conduction — is accompanied by a step change of the contact temperature at the initial time. Another finding is that the initial heat partition occurs due to the ratio of $K_1\sqrt{\alpha_1/k_1}$ and $K_2\sqrt{\alpha_2/k_2}$ under Jeffreys heat conduction and due to the different ratio of $K_1/\sqrt{k_1\tau_1}$ and $K_2/\sqrt{k_2\tau_2}$ under Cattaneo heat conduction. The solution applicability was demonstrated on the simulation example of ultrashort laser pulse welding. The type of heat conduction was revealed to have qualitative and quantitative impacts on the contact temperature and heat fluxes.

Notation

c_v	volumetric heat capacity, J/(m^3 °C)
k	thermal diffusivity, $k = K/c_\mathrm{v}$, m^2/s
q	heat flux, W/m^2
$\bar{q}$	heat flux vector, W/m^2
q_0	maximum value of specific power q_s, W/m^2
q_s	specific power of heat source, W/m^2
s	Laplace transform parameter
t	time variable, s
t_s	heating duration, s
x	spatial coordinate, m
$I_0(\cdot)$	modified Bessel function of first kind and zero order
K	thermal conductivity, W/(m °C)
Q	dimensionless heat flux, $Q = q/q_0$
Q_s	dimensionless specific power of heat source, $Q_\mathrm{s} = q_\mathrm{s}/q_0$
T	temperature, °C
T_0	initial temperature, °C
α	relative contribution of Fourier heat conduction
$\delta(\cdot)$	Dirac delta function
η	dimensionless time variable, $\eta = t/\tau_1$
ϑ	dimensionless temperature, $\vartheta = K_1(T - T_0)/\left(q_0\sqrt{k_1\tau_1}\right)$
ξ	dimensionless spatial coordinate, $\xi = x/\sqrt{k_1\tau_1}$
τ	thermal relaxation time, s
χ	thermal diffusivity ratio, $\chi = k_2/k_1$
$\Gamma(\cdot)$	gamma function
$\Gamma(\cdot,\cdot)$	upper incomplete gamma function
Θ	thermal relaxation time ratio, $\Theta = \tau_2/\tau_1$
Λ	thermal conductivity ratio, $\Lambda = K_2/K_1$
$\mathcal{L}[\cdot]$	Laplace transform operator
∇	operator nabla
$\widetilde{\blacksquare}$	Laplace transform image
$\blacksquare_1$	related to semispace 1
$\blacksquare_2$	related to semispace 2
$\blacksquare_{1,2}$	related to semispaces 1 and 2
$\blacksquare_\mathrm{c}$	related to contact region $x = 0$
$\blacksquare_\mathrm{C}$	related to Cattaneo heat conduction
$\blacksquare_\mathrm{F}$	related to Fourier heat conduction

1. Introduction

Heat conduction is one of the basic mechanisms of transfer of heat energy between bodies being in mechanical contact. The problems of contact heat conduction represent an important class of heat transfer problems often met in different branches of science, engineering and technology. Analysis of heat conduction in coupled bodies presents serious difficulties compared to that for a single body due to the necessity of taking account of the properties of both bodies and contact conditions.

The classical law of heat flux introduced by Fourier [1] states that heat flux $\bar{q}_{\mathrm{F}}$ in a conductive medium is proportional in its magnitude to the gradient of temperature T and has the opposite direction, i.e.

$$\bar{q}_{\mathrm{F}} = -K_{\mathrm{F}} \nabla T \tag{1}$$

Here ∇ is the operator nabla; K_{F} is the Fourier thermal conductivity. The statement of heat energy conservation and Eq.(1) lead to the parabolic heat conduction equation (diffusion equation) in the form

$$\frac{\partial T}{\partial t} = k_{\mathrm{F}} \nabla^2 T \tag{2}$$

where t is the time variable; k_{F} is the Fourier thermal diffusivity. Eq.(2) has served as the basis for a great number of contact heat conduction studies. Some of the earliest studies were published in the first half of the 20th century, e.g. Carslaw [2], Mersman [3] and Schaaf [4].

In accordance with the Fourier heat flux law of Eq.(1), heat propagates in a medium at infinite speed. If the temperature at some point undergoes a sudden change, there will be an instantaneous temperature response at any finite distance from this point. This, however, contradicts the experiments revealing finiteness of the heat propagation speed for liquid helium (Peshkov [5]) and dielectric crystals (Ackerman et al. [6]) at low temperatures.

Based on the studies by Maxwell [7], Landau [8], Cattaneo [9], Vernotte [10] and others, an alternative concept was proposed introducing the heat flux inertia effect and stating that heat is transmitted by waves at finite speeds. The corresponding heat flux equation is represented in the form

$$\tau \frac{\partial \bar{q}_{\mathrm{C}}}{\partial t} + \bar{q}_{\mathrm{C}} = -K_{\mathrm{C}} \nabla T \tag{3}$$

where τ is the thermal relaxation time. The statement of heat energy conservation and Eq.(3) imply the hyperbolic heat conduction equation (damped wave equation) as follows:

$$\tau \frac{\partial^2 T}{\partial t^2} + \frac{\partial T}{\partial t} = k_{\mathrm{C}} \nabla^2 T \tag{4}$$

Following Joseph and Preziosi [11], Eq.(4) is referred to as 'Cattaneo heat conduction equation' in the present study, without meaning to downplay the contributions of the other scientists. The related quantities have subscript 'C'.

Cattaneo heat conduction in coupled bodies has been studied for different boundary and initial conditions, as reviewed next. Kazimi and Erdman [12] investigated the influence of initial temperature difference of coupled semispaces on their contact temperature behaviour. Frankel et al. [13] investigated temperatures and heat fluxes in a system of layers affected by volumetric heat sources. Tzou [14] performed harmonic analysis of the reflection and refraction of thermal waves from the interface between dissimilar materials. Lor and Chu [15, 16] investigated the influence of a pulsed external heat source on temperatures and heat fluxes in two layers coupled with a radiation contact condition. Duhamel [17] investigated heat conduction in heterogeneous media using a finite integral transform technique. Khadrawi et al. [18] investigated temperatures in two layers in imperfect thermal contact subjected to a rapid temperature change at an external surface. Tsai and Hung [19] investigated the thermal behaviour of a bi-layered sphere due to a rapid temperature change at the external surface. Dai and Niu [20, 21] developed finite difference schemes for studying temperatures in two coupled layers with temperature-dependent properties exposed to a volumetric heat source. Ordóñez-Miranda and Alvarado-Gil [22] investigated thermal waves in coupled layer and semispace excited by a modulated external heat source. Nosko [23] investigated contact temperature and heat fluxes in coupled semispaces subjected to an interfacial heat source.

The experimental results related to the detection of second sound and ballistic transport in solids at low temperatures (Ackerman and Guyer [24], McNelly et al. [25]) and extremely fast heating of solids by laser pulses at room temperature (Li et al. [26], Jiang [27], Banerjee et al. [28]) call for non-Fourier models generalising the parabolic and hyperbolic types of heat conduction. A mathematically simple approach is to assume that the Fourier heat flux $\bar{q}_{\mathrm{F}}$ obeys Eq.(1) as

$$\bar{q}_{\mathrm{F}} = -K_{\mathrm{F}} \nabla T = -\alpha K \nabla T$$

whilst the Cattaneo heat flux $\bar{q}_{\mathrm{C}}$ obeys Eq.(3) as

$$\tau \frac{\partial \bar{q}_{\mathrm{C}}}{\partial t} + \bar{q}_{\mathrm{C}} = -K_{\mathrm{C}} \nabla T = -(1-\alpha) K \nabla T$$

and, in addition, the total heat flux $\bar{q}$ is the sum of $\bar{q}_{\mathrm{F}}$ and $\bar{q}_{\mathrm{C}}$, i.e. $\bar{q} = \bar{q}_{\mathrm{F}} + \bar{q}_{\mathrm{C}}$. Here $K = K_{\mathrm{F}} + K_{\mathrm{C}}$ is the total thermal conductivity and $\alpha = K_{\mathrm{F}}/(K_{\mathrm{F}} + K_{\mathrm{C}})$ is the coefficient indicating the relative contribution of Fourier heat conduction. Then the relationship between the total heat flux $\bar{q}$ and temperature T is described by the Jeffreys heat flux equation in the form (Tamma and Zhou [29])

$$\tau \frac{\partial \bar{q}}{\partial t} + \bar{q} = -K\nabla T - \alpha\tau K \frac{\partial(\nabla T)}{\partial t} \tag{5}$$

Combination of Eq.(5) and the statement of heat energy conservation

$$c_{\mathrm{v}} \frac{\partial T}{\partial t} + \nabla \cdot \bar{q} = 0$$

leads to the heat conduction equation

$$\tau \frac{\partial^2 T}{\partial t^2} + \frac{\partial T}{\partial t} = k\nabla^2 T + \alpha\tau k \frac{\partial(\nabla^2 T)}{\partial t} \tag{6}$$

where c_{v} is the volumetric heat capacity; $k = K/c_{\mathrm{v}}$ is the total thermal diffusivity. Apparently, the particular cases of Eq.(6) include Fourier heat conduction of Eq.(2) at $K_{\mathrm{C}} = 0$ and Cattaneo heat conduction of Eq.(4) at $K_{\mathrm{F}} = 0$.

It is important to note that the one-dimensional representation of Eq.(6) is practically equivalent to the Guyer-Krumhansl equation

$$\tau \frac{\partial^2 T}{\partial t^2} + \frac{\partial T}{\partial t} = k \frac{\partial^2 T}{\partial x^2} + l^2 \frac{\partial^3 T}{\partial x^2 \partial t}$$

developed from the linearised phonon Boltzmann equation [30], under the condition that the dissipation parameter l^2 related to the mean free path equals $\alpha\tau k$. The Guyer-Krumhansl equation is consistent with the kinetic theory and second law of thermodynamics if the parameters k, τ and l^2 take positive values (Fehér and Kovács [31], Ramos et al. [32]), which, in fact, does not impose extra limitations on the parameters k, τ and α incorporated in Eq.(6). Moreover, the experimental studies by Both et al. [33] and Ván et al. [34] claim that the Guyer-Krumhansl equation allows more accurate temperature simulations compared to Fourier heat conduction of Eq.(2) for the case of heterogeneous materials like rocks and foams at room temperature.

Another important remark is that Eq.(6) can be considered as the first-order approximation of a dual-phase-lag model by Tzou [35] formulated with respect to T as

$$\tau \frac{\partial^2 T}{\partial t^2} + \frac{\partial T}{\partial t} = k \frac{\partial^2 T}{\partial x^2} + k\tau_T \frac{\partial^3 T}{\partial x^2 \partial t}$$

under the condition that the temperature gradient phase lag τ_T equals $\alpha\tau$. The dual-phase-lag model gained popularity in the heat conduction literature, despite the criticism of violating basic physical principles (Fabrizio and Lazzari [36], Rukolaine [37], Awad [38]).

The contact heat conduction problems based on the dual-phase-lag and Jeffreys models have been reported. Ho et al. [39] performed a numerical study of heat conduction in a system of layers using a lattice Boltzmann method. Al-Nimr et al. [40] investigated temperature responses in two layers due to harmonic excitation in the form of a volumetric heat source in one of the layers or

temperature variation at an external surface. Al-Huniti and Al-Nimr [41] investigated the thermoelastic behaviour of two layers subjected to a rapid temperature change at an external surface using the Laplace transform technique along with a numerical procedure based on a Riemann-sum approximation. A similar approach was applied by Lee and Tsai [42] who investigated the pulsed volumetric heating of a layer and a semispace in imperfect thermal contact and Ramadan [43] who investigated the pulsed heating of a multi-layer system by an external heat flux. Ramadan and Al-Nimr [44] performed numerical simulations of the thermal behaviour of two layers in imperfect thermal contact with different initial temperatures. Akbarzadeh and Pasini [45] investigated the thermal response of a system of layers in imperfect thermal contact to temperature variations at the external surfaces using the Laplace transform and fast inverse Laplace transform techniques. Yeoh et al. [46] applied a finite difference method with high-order total variation diminishing schemes to simulate temperatures in a multi-layer system. Xue et al. [47, 48] investigated heat conduction in two layers in imperfect thermal contact using an original differential-algebraic equation time integration framework.

Analysis shows that the studies mentioned above do not cover the Jeffreys heat conduction problem for two coupled bodies heated by an interfacial heat source. This problem may arise in practically important applications, such as laser processing of materials (Ma et al. [49]), simulations of heat transfer in biological tissues (Xu et al. [50]), simulations of microscopic frictional processes (Nosko [51]) and other applications involving instantaneous interactions of mechanical, electromagnetic or chemical nature. Moreover, the majority of the studies employ numerical or semi-analytical methods to find temperature and heat flux solutions and, therefore, these solutions are unsuitable for accurate asymptotic and parametric analysis. The purpose of the present study was to find an analytical solution of the Jeffreys heat conduction problem for coupled semispaces subjected to the action of an interfacial heat source of variable specific power and analyse the solution in terms of asymptotic behaviour, parametric sensitivity and potential applications.

2. Problem definition and governing equations

A schematic of the studied contact heat conduction problem is presented in Fig.1. Consider the semispaces 1 and 2 which occupy the respective domains $x > 0$ and $x < 0$. Assume that temperatures $T_{1,2}(x,t)$ in the semispaces satisfy Eq.(6), implying the following heat conduction equations:

$$\tau_1 \frac{\partial^2 T_1}{\partial t^2} + \frac{\partial T_1}{\partial t} = k_1 \frac{\partial^2 T_1}{\partial x^2} + \alpha_1 \tau_1 k_1 \frac{\partial^3 T_1}{\partial x^2 \partial t}, \qquad x > 0, \qquad t > 0;$$

$$\tau_2 \frac{\partial^2 T_2}{\partial t^2} + \frac{\partial T_2}{\partial t} = k_2 \frac{\partial^2 T_2}{\partial x^2} + \alpha_2 \tau_2 k_2 \frac{\partial^3 T_2}{\partial x^2 \partial t}, \qquad x < 0, \qquad t > 0$$

(7)

where $k_{1,2}$ are the thermal diffusivities; $\tau_{1,2}$ are the thermal relaxation times; $\alpha_{1,2}$ are the coefficients indicating the relative contribution of Fourier heat conduction.

At the initial time $t = 0$, the temperatures $T_{1,2}$ are uniformly distributed and equal between each other, i.e.

$$T_1|_{t=0} = T_2|_{t=0} = T_0$$

(8)

and their derivatives with respect to the time variable t equal zero:

$$\left.\frac{\partial T_1}{\partial t}\right|_{t=0} = \left.\frac{\partial T_2}{\partial t}\right|_{t=0} = 0$$

(9)

where T_0 is the initial temperature.

Temperature continuity is assumed in the contact region $x = 0$ between the semispaces:

$$T_1|_{x=0} = T_2|_{x=0} = T_\mathrm{c}$$

(10)

Here $T_\mathrm{c}(t)$ denotes the contact temperature.

Heat fluxes $q_{1,2}(x,t)$ in the semispaces are coupled via the interfacial heat source acting with variable specific power $q_\mathrm{s}(t)$ in the form of a polynomial

$$q_1|_{x=0} - q_2|_{x=0} = q_\mathrm{s} = q_0 \sum_{i=0}^{n} p_i t^i$$

(11)

where q_0 is the maximum value of q_s in the considered time interval from zero to t_s; n is the degree of the polynomial; p_i is the i-th coefficient of the polynomial. The contact heat fluxes are further denoted by $q_{\mathrm{c}1,2}(t) = \left.q_{1,2}\right|_{x=0}$.

The relationship between $q_{1,2}$ and $T_{1,2}$ is defined by Eq.(5) as follows:

$$\begin{aligned}\tau_1 \frac{\partial q_1}{\partial t} + q_1 &= -K_1 \frac{\partial T_1}{\partial x} - \alpha_1 \tau_1 K_1 \frac{\partial^2 T_1}{\partial x \partial t};\\ \tau_2 \frac{\partial q_2}{\partial t} + q_2 &= -K_2 \frac{\partial T_2}{\partial x} - \alpha_2 \tau_2 K_2 \frac{\partial^2 T_2}{\partial x \partial t}\end{aligned}$$

(12)

where $K_{1,2}$ are the thermal conductivities.

The problem definition becomes complete by specifying the conditions of zero disturbance at infinite distance from the contact region:

$$\left.\frac{\partial T_1}{\partial x}\right|_{x\to+\infty} = \left.\frac{\partial T_2}{\partial x}\right|_{x\to-\infty} = 0$$

(13)

The problem of Eqs.(7)–(13) should be represented in the dimensionless form to decrease the number of parameters and simplify analysis. Dimensionless spatial coordinate ξ, time variable η, temperatures $\vartheta_{1,2}$, contact temperature ϑ_{c}, heat fluxes $Q_{1,2}$, contact heat fluxes $Q_{\mathrm{c}1,2}$ and heat source specific power Q_{s} are introduced as follows:

$$\xi = \frac{x}{\sqrt{k_1\tau_1}}, \qquad \eta = \frac{t}{\tau_1},$$

$$\vartheta_{1,2} = \frac{K_1\left(T_{1,2} - T_0\right)}{q_0\sqrt{k_1\tau_1}}, \qquad \vartheta_{\mathrm{c}} = \frac{K_1(T_{\mathrm{c}} - T_0)}{q_0\sqrt{k_1\tau_1}},$$

$$Q_{1,2} = \frac{q_{1,2}}{q_0}, \qquad Q_{\mathrm{c}1,2} = \frac{q_{\mathrm{c}1,2}}{q_0}, \qquad Q_s = \frac{q_{\mathrm{s}}}{q_0}$$

The dimensionless parameters include the coefficients $\alpha_{1,2}$ and thermal conductivity ratio Λ, thermal diffusivity ratio χ, thermal relaxation time ratio Θ given by

$$\Lambda = \frac{K_2}{K_1}, \qquad \chi = \frac{k_2}{k_1}, \qquad \Theta = \frac{\tau_2}{\tau_1}$$

and polynomial coefficients

$$\mu_i = p_i\tau_1^i, \qquad i = 0, \ldots, n$$

Finally, the dimensionless variables and parameters above lead to the problem definition incorporating the heat conduction equations

$$\frac{\partial^2\vartheta_1}{\partial\eta^2} + \frac{\partial\vartheta_1}{\partial\eta} = \frac{\partial^2\vartheta_1}{\partial\xi^2} + \alpha_1\frac{\partial^3\vartheta_1}{\partial\xi^2\partial\eta};$$

$$\Theta\frac{\partial^2\vartheta_2}{\partial\eta^2} + \frac{\partial\vartheta_2}{\partial\eta} = \chi\frac{\partial^2\vartheta_2}{\partial\xi^2} + \alpha_2\chi\Theta\frac{\partial^3\vartheta_2}{\partial\xi^2\partial\eta}$$

(14)

initial conditions

$$\vartheta_1|_{\eta=0} = \vartheta_2|_{\eta=0} = 0;$$

$$\left.\frac{\partial\vartheta_1}{\partial\eta}\right|_{\eta=0} = \left.\frac{\partial\vartheta_2}{\partial\eta}\right|_{\eta=0} = 0$$

(15)

temperature continuity condition

$$\vartheta_1|_{\xi=0} = \vartheta_2|_{\xi=0} = \vartheta_{\mathrm{c}}$$

(16)

heat source condition

$$Q_1|_{\xi=0} - Q_2|_{\xi=0} = Q_{\mathrm{s}} = \sum_{i=0}^{n}\mu_i\eta^i$$

(17)

keeping in mind that

$$\frac{\partial Q_1}{\partial \eta} + Q_1 = -\frac{\partial \vartheta_1}{\partial \xi} - \alpha_1 \frac{\partial^2 \vartheta_1}{\partial \xi \partial \eta};$$

$$\Theta \frac{\partial Q_2}{\partial \eta} + Q_2 = -\Lambda \frac{\partial \vartheta_2}{\partial \xi} - \alpha_2 \Lambda \Theta \frac{\partial^2 \vartheta_2}{\partial \xi \partial \eta}$$

(18)

and conditions of zero disturbance at infinity

$$\left.\frac{\partial \vartheta_1}{\partial \xi}\right|_{\xi \to +\infty} = \left.\frac{\partial \vartheta_2}{\partial \xi}\right|_{\xi \to -\infty} = 0$$

(19)

The problem of Eqs.(14)–(19) is solved and analysed in the following sections.

3. Problem solution using the Laplace transform approach

Apply the Laplace transform $\tilde{g}(s) = \mathcal{L}[g(\eta)]$ with respect to the time variable η (Doetsch [52]). Here s is the transform parameter. The temperature images $\tilde{\vartheta}_{1,2}(\xi, s)$ are then found from Eq.(14) with account of zero initial conditions of Eq.(15) as follows:

$$(\alpha_1 s + 1) \frac{\partial^2 \tilde{\vartheta}_1}{\partial \xi^2} - s(s+1)\tilde{\vartheta}_1 = 0;$$

$$\chi(\alpha_2 \Theta s + 1) \frac{\partial^2 \tilde{\vartheta}_2}{\partial \xi^2} - s(\Theta s + 1)\tilde{\vartheta}_2 = 0$$

(20)

The solution of Eq.(20) that satisfies the temperature continuity condition of Eq.(16) and zero disturbance conditions of Eq.(19) is found in the form

$$\tilde{\vartheta}_1 = \tilde{\vartheta}_c \exp\left\{-\xi \sqrt{\frac{s(s+1)}{\alpha_1 s + 1}}\right\};$$

$$\tilde{\vartheta}_2 = \tilde{\vartheta}_c \exp\left\{\frac{\xi}{\sqrt{\chi}} \sqrt{\frac{s(\Theta s + 1)}{\alpha_2 \Theta s + 1}}\right\}$$

(21)

where $\tilde{\vartheta}_c(s)$ is a yet unknown image of the contact temperature $\vartheta_c(\eta)$.

The heat flux images $\tilde{Q}_{1,2}(\xi, s)$ are determined from Eq.(18) and represented as

$$\tilde{Q}_1 = -\frac{\alpha_1 s + 1}{s + 1} \frac{\partial \tilde{\vartheta}_1}{\partial \xi};$$

$$\tilde{Q}_2 = -\Lambda \frac{\alpha_2 \Theta s + 1}{\Theta s + 1} \frac{\partial \tilde{\vartheta}_2}{\partial \xi} \tag{22}$$

Further, substitute Eq.(21) and Eq.(22) into Eq.(17) in the space of images and obtain the contact temperature image

$$\begin{aligned} \tilde{\vartheta}_{\mathrm{c}} &= \frac{\sqrt{\chi}\sqrt{\Theta s + 1}\sqrt{s+1}}{\sqrt{\chi}\sqrt{\alpha_1 s + 1}\sqrt{\Theta s + 1} + \Lambda\sqrt{\alpha_2 \Theta s + 1}\sqrt{s+1}} \sum_{i=0}^{n} \frac{i!\,\mu_i}{s^{3/2+i}} \\ &= \frac{\sqrt{\chi}}{\alpha_1\chi - \alpha_2\Lambda^2} \left(\sqrt{\alpha_1 \chi} \frac{(s+\Theta^{-1})\sqrt{s+1}\sqrt{s+\alpha_1^{-1}}}{(s-a_1)(s-a_2)} \right. \\ &\quad \left. - \Lambda\sqrt{\alpha_2} \frac{(s+1)\sqrt{s+\Theta^{-1}}\sqrt{s+\alpha_2^{-1}\Theta^{-1}}}{(s-a_1)(s-a_2)} \right) \sum_{i=0}^{n} \frac{i!\,\mu_i}{s^{3/2+i}} \end{aligned} \tag{23}$$

where

$$a_{1,2} = -\frac{\alpha_1\chi - \alpha_2\Lambda^2\Theta + \chi\Theta - \Lambda^2}{2\Theta(\alpha_1\chi - \alpha_2\Lambda^2)} \pm \frac{\sqrt{(\alpha_1\chi - \alpha_2\Lambda^2\Theta + \chi\Theta - \Lambda^2)^2 - 4\Theta(\alpha_1\chi - \alpha_2\Lambda^2)(\chi - \Lambda^2)}}{2\Theta(\alpha_1\chi - \alpha_2\Lambda^2)}$$

The contact heat flux images $\tilde{Q}_{\mathrm{c}1,2}(s)$ can be expressed based on Eqs.(21)–(23) as

$$\begin{aligned} \tilde{Q}_{\mathrm{c}1} &= \frac{\sqrt{\alpha_1\chi}}{\alpha_1\chi - \alpha_2\Lambda^2} \left(\sqrt{\alpha_1\chi} \frac{(s+\Theta^{-1})(s+\alpha_1^{-1})}{(s-a_1)(s-a_2)} \right. \\ &\quad \left. - \Lambda\sqrt{\alpha_2} \frac{\sqrt{s+1}\sqrt{s+\Theta^{-1}}\sqrt{s+\alpha_1^{-1}}\sqrt{s+\alpha_2^{-1}\Theta^{-1}}}{(s-a_1)(s-a_2)} \right) \sum_{i=0}^{n} \frac{i!\,\mu_i}{s^{1+i}}; \\ \tilde{Q}_{\mathrm{c}2} &= \frac{\Lambda\sqrt{\alpha_2}}{\alpha_1\chi - \alpha_2\Lambda^2} \left(\Lambda\sqrt{\alpha_2} \frac{(s+1)(s+\alpha_2^{-1}\Theta^{-1})}{(s-a_1)(s-a_2)} \right. \\ &\quad \left. - \sqrt{\alpha_1\chi} \frac{\sqrt{s+1}\sqrt{s+\Theta^{-1}}\sqrt{s+\alpha_1^{-1}}\sqrt{s+\alpha_2^{-1}\Theta^{-1}}}{(s-a_1)(s-a_2)} \right) \sum_{i=0}^{n} \frac{i!\,\mu_i}{s^{1+i}} \end{aligned} \tag{24}$$

The property of linearity and known Laplace transforms (Carslaw and Jaeger [53]) yield that

$$\mathcal{L}^{-1}\left[\frac{1}{\sqrt{s+b}\sqrt{s+c}}\right] = \phi(\eta, b, c) = \exp\left\{-\frac{b+c}{2}\eta\right\} I_0\left(\frac{b-c}{2}\eta\right);$$

$$\begin{aligned} \mathcal{L}^{-1}\left[\frac{(s+b)(s+c)}{(s-a_1)(s-a_2)s^{1+i}}\right] &= \varrho(\eta, i, b, c) \\ &= \frac{(a_1+b)(a_1+c)}{a_1^{1+i}(a_1-a_2)} \exp\{a_1\eta\}\left(1 - \frac{\Gamma(1+i, a_1\eta)}{i!}\right) \\ &\quad + \frac{(a_2+b)(a_2+c)}{a_2^{1+i}(a_2-a_1)} \exp\{a_2\eta\}\left(1 - \frac{\Gamma(1+i, a_2\eta)}{i!}\right) + \frac{\eta^i}{i!}; \end{aligned}$$

$$\mathcal{L}^{-1}\left[\frac{(s+b)(s+c)(s+d)}{(s-a_1)(s-a_2)s^{3/2+i}}\right]=\lambda(\eta,i,b,c,d)$$
$$=\frac{(a_1+b)(a_1+c)(a_1+d)}{a_1^{3/2+i}(a_1-a_2)}\exp\{a_1\eta\}\left(1-\frac{\Gamma(3/2+i,a_1\eta)}{\Gamma(3/2+i)}\right)$$
$$+\frac{(a_2+b)(a_2+c)(a_2+d)}{a_2^{3/2+i}(a_2-a_1)}\exp\{a_2\eta\}\left(1-\frac{\Gamma(3/2+i,a_2\eta)}{\Gamma(3/2+i)}\right)$$
$$+\frac{a_1+a_2+b+c+d}{\Gamma(3/2+i)}\eta^{i+1/2}+\frac{1/2+i}{\Gamma(3/2+i)}\eta^{i-1/2};$$

$$\mathcal{L}^{-1}\left[\frac{(s+b)(s+c)(s+d)(s+f)}{(s-a_1)(s-a_2)s^{1+i}}\right]=\kappa(\eta,i,b,c,d,f)$$
$$=\frac{(a_1+b)(a_1+c)(a_1+d)(a_1+f)}{a_1^{1+i}(a_1-a_2)}\exp\{a_1\eta\}\left(1-\frac{\Gamma(i,a_1\eta)}{\Gamma(i)}\right)$$
$$+\frac{(a_2+b)(a_2+c)(a_2+d)(a_2+f)}{a_2^{1+i}(a_2-a_1)}\exp\{a_2\eta\}\left(1-\frac{\Gamma(i,a_2\eta)}{\Gamma(i)}\right)+\frac{bcdf}{i!\,a_1a_2}\eta^i$$
$$+(a_1+a_2+b+c+d+f)\begin{cases}\delta(\eta), & i=0;\\ \dfrac{\eta^{i-1}}{(i-1)!}, & i=1,2,\ldots\end{cases}+\begin{cases}\delta'^{(\eta)}, & i=0;\\ \delta(\eta), & i=1;\\ \dfrac{\eta^{i-2}}{(i-2)!}, & i=2,3,\ldots\end{cases}$$

(25)

where b, c, d and f are positive real numbers; I_0 is the modified Bessel function of the first kind and zero order; $\Gamma(\cdot)$ is the gamma function; $\Gamma(\cdot,\cdot)$ is the upper incomplete gamma function; $\delta(\cdot)$ is the Dirac delta function.

The convolution theorem and the transforms given by Eq.(25) allow representing the original of Eq.(23) in the form

$$\vartheta_{\mathrm{c}}=\frac{\sqrt{\chi}}{\alpha_1\chi-\alpha_2\Lambda^2}\sum_{i=0}^{n}(i!\,\mu_i)\int_0^{\eta}\Big(\sqrt{\alpha_1\chi}\,\phi(\eta-\varsigma,1,\alpha_1^{-1})\lambda(\varsigma,i,1,\alpha_1^{-1},\Theta^{-1})$$
$$-\Lambda\sqrt{\alpha_2}\,\phi(\eta-\varsigma,\Theta^{-1},\alpha_2^{-1}\Theta^{-1})\lambda(\varsigma,i,\Theta^{-1},\alpha_2^{-1}\Theta^{-1},1)\Big)\,d\varsigma$$

(26)

and the originals of Eq.(24) in the form

$$Q_{\mathrm{c1}}=\frac{\sqrt{\alpha_1\chi}}{\alpha_1\chi-\alpha_2\Lambda^2}\sum_{i=0}^{n}(i!\,\mu_i)\Bigg(\sqrt{\alpha_1\chi}\,\varrho(\eta,i,\Theta^{-1},\alpha_1^{-1})$$
$$-\Lambda\sqrt{\alpha_2}\int_0^{\eta}\phi(\eta$$
$$-\varsigma,1,\Theta^{-1})\int_0^{\varsigma}\phi(\varsigma-\epsilon,\alpha_1^{-1},\alpha_2^{-1}\Theta^{-1})\kappa(\epsilon,i,1,\Theta^{-1},\alpha_1^{-1},\alpha_2^{-1}\Theta^{-1})\,d\epsilon d\varsigma\Bigg);$$

$$Q_{c2} = \frac{\Lambda\sqrt{\alpha_2}}{\alpha_1\chi - \alpha_2\Lambda^2}\sum_{i=0}^{n}(i!\,\mu_i)\left(\Lambda\sqrt{\alpha_2}\,\varrho(\eta, i, 1, \alpha_2^{-1}\Theta^{-1})\right.$$
$$- \sqrt{\alpha_1\chi}\int_0^{\eta}\phi(\eta$$
$$\left. - \varsigma, 1, \Theta^{-1})\int_0^{\varsigma}\phi(\varsigma - \epsilon, \alpha_1^{-1}, \alpha_2^{-1}\Theta^{-1})\kappa(\epsilon, i, 1, \Theta^{-1}, \alpha_1^{-1}, \alpha_2^{-1}\Theta^{-1})\,d\epsilon d\varsigma\right) \tag{27}$$

Thereby, the contact temperature ϑ_c and heat fluxes $Q_{c1,2}$ can be determined using respective Eq.(26) and Eq.(27). Note that finding the analytical expressions of the temperature distributions $\vartheta_{1,2}$ requires inversion of Eq.(21) which is cumbersome. The relevant mathematical approaches are discussed in Awad et al. [54].

4. Solution validation

The solution given by Eq.(26) and Eq.(27) is validated by its comparisons to the known analytical expressions and numerically calculated values. Fig.2 shows an example of such a comparison for the contact temperature ϑ_c and heat flux Q_{c1}. In the case of $\alpha_1 = \alpha_2 = 1$, the Fourier heat flux law of Eq.(1) takes place, and the solution coincides with the expressions for parabolic heat conduction in coupled semispaces (Carslaw and Jaeger [53]). In the opposite case, at $\alpha_1 = \alpha_2 = 0$, the heat flux and temperature are related due to the Cattaneo heat flux law of Eq.(3), and the solution degenerates to that derived by Nosko [23] for the problem of hyperbolic heat conduction in coupled semispaces. In the general case, when the heat conduction is governed by the Jeffreys heat flux law of Eq.(5), i.e. the coefficients $\alpha_{1,2}$ take arbitrary values in between zero and unit, the validation is performed using a numerical algorithm.

The algorithm is developed based on the implicit Backward Time Centered Space method (BTCS). The validation of the algorithm itself includes comparisons of the numerical results to those obtained by other finite difference approximations, e.g. the Crank-Nicolson implicit method (CN). Fig.3 shows a small portion of the validation procedure on the example of calculation of the spatial temperature distributions $\vartheta_{1,2}$. A perfect match is seen between the values obtained by BTCS and CN and between these values and the mentioned analytical expressions for the Fourier and Cattaneo types of heat conduction. It is also seen that the algorithm allows accurate simulation of the thermal waves with sharp fronts intrinsic to Cattaneo heat conduction of Eq.(4) (Özişik and Tzou [55]). An accuracy of 6 significant digits is achieved at the number of spatial and time discretisation steps of order 10^3.

5. Asymptotic analysis

The asymptotic behaviour of the contact temperature ϑ_c and heat flux Q_{c1} is analysed for the heat source of constant specific power $Q_s = 1$, i.e. $n = 0$ and $\mu_0 = 1$ are specified in Eq.(17). Since the image functions given by Eq.(23) and Eq.(24) are substantially simpler compared to the original functions given by Eq.(26) and Eq.(27), it is reasonable to make use of the relationship between the limit behaviour of an original function and that of the corresponding image function (Doetsch [52]).

First consider the case of small time variable η. The limit expressions of Eq.(23) and Eq.(24) at real-valued $s \to \infty$ read

$$\tilde{\vartheta}_c \cong \frac{\sqrt{\chi}}{(\sqrt{\chi\alpha_1} + \Lambda\sqrt{\alpha_2})s\sqrt{s}} \tag{28}$$

and

$$\tilde{Q}_{c1} \cong \frac{\sqrt{\chi\alpha_1}}{(\sqrt{\chi\alpha_1} + \Lambda\sqrt{\alpha_2})s} \tag{29}$$

Of particular interest is Cattaneo heat conduction that takes place at $\alpha_1 = \alpha_2 = 0$. Simplification of Eq.(21) and Eq.(22) and their substitution into Eq.(17) in the space of images lead to the image functions

$$\tilde{\vartheta}_c = \frac{\sqrt{\chi\Theta}\sqrt{s+1}\sqrt{s+\Theta^{-1}}}{s\sqrt{s}\left(\Lambda\sqrt{s+1} + \sqrt{\chi\Theta}\sqrt{s+\Theta^{-1}}\right)};$$

$$\tilde{Q}_{c1} = \frac{\sqrt{\chi\Theta}\sqrt{s+\Theta^{-1}}}{s\left(\Lambda\sqrt{s+1} + \sqrt{\chi\Theta}\sqrt{s+\Theta^{-1}}\right)}$$

which at real-valued $s \to \infty$ are asymptotically equivalent to

$$\tilde{\vartheta}_c \cong \tilde{Q}_{c1} \cong \frac{\sqrt{\chi\Theta}}{\left(\Lambda + \sqrt{\chi\Theta}\right)s} \tag{30}$$

Finally, inversion of Eqs.(28)–(30) results in the limit expressions for $\eta \to 0$ as follows:

$$\vartheta_c \cong \begin{cases} \dfrac{2\sqrt{\chi}}{\sqrt{\pi}(\sqrt{\chi\alpha_1} + \Lambda\sqrt{\alpha_2})}\sqrt{\eta}, & \alpha_1 \neq 0 \text{ or } \alpha_2 \neq 0; \\ \dfrac{\sqrt{\chi\Theta}}{\Lambda + \sqrt{\chi\Theta}}, & \alpha_1 = \alpha_2 = 0 \end{cases} \tag{31}$$

and

$$Q_{c1} \cong \begin{cases} \dfrac{\sqrt{\chi\alpha_1}}{\sqrt{\chi\alpha_1}+\Lambda\sqrt{\alpha_2}}, & \alpha_1 \neq 0 \text{ or } \alpha_2 \neq 0; \\ \dfrac{\sqrt{\chi\Theta}}{\Lambda+\sqrt{\chi\Theta}}, & \alpha_1 = \alpha_2 = 0 \end{cases} \tag{32}$$

It is remarkable that under Cattaneo heat conduction at $\alpha_1 = \alpha_2 = 0$, the initial rise of ϑ_c is equal to that of Q_{c1}.

Represent Eq.(31) and Eq.(32) in the dimensional form

$$T_c - T_0 \cong \begin{cases} \dfrac{2q_0\sqrt{t}}{\sqrt{\pi}\left(K_1\sqrt{\alpha_1/k_1}+K_2\sqrt{\alpha_2/k_2}\right)}, & \alpha_1 \neq 0 \text{ or } \alpha_2 \neq 0; \\ \dfrac{q_0}{K_1/\sqrt{k_1\tau_1}+K_2/\sqrt{k_2\tau_2}}, & \alpha_1 = \alpha_2 = 0 \end{cases} \tag{33}$$

and

$$q_{c1} \cong \begin{cases} \dfrac{K_1\sqrt{\alpha_1/k_1}}{K_1\sqrt{\alpha_1/k_1}+K_2\sqrt{\alpha_2/k_2}}q_0, & \alpha_1 \neq 0 \text{ or } \alpha_2 \neq 0; \\ \dfrac{K_1/\sqrt{k_1\tau_1}}{K_1/\sqrt{k_1\tau_1}+K_2/\sqrt{k_2\tau_2}}q_0, & \alpha_1 = \alpha_2 = 0 \end{cases} \tag{34}$$

In accordance with Eq.(33) and Eq.(34), under Jeffreys heat conduction at $\alpha_1 \neq 0$ or $\alpha_2 \neq 0$, the relative contact temperature $(T_c - T_0)$ increases continuously as $\sqrt{t}$, whilst the generated heat is partitioned between the semispaces due to the ratio of $K_1\sqrt{\alpha_1/k_1}$ and $K_2\sqrt{\alpha_2/k_2}$. Note that the expressions of T_c and q_{c1} are independent of τ_1 and τ_2. Thereby, the Fourier component of heat conduction predominates over the Cattaneo component as regards the qualitative behaviour of T_c and q_{c1}, which is in line with the discussions by Tamma and Zhou [29].

Cattaneo heat conduction at $\alpha_1 = \alpha_2 = 0$ is characterised by a step change of T_c that depends on the parameters $K_{1,2}$, $k_{1,2}$ and $\tau_{1,2}$. Fig.4 illustrates the dimensionless dependence of the initial rise of ϑ_c on the parameter Λ and product $\chi\Theta$ due to Eq.(31). It is seen that ϑ_c decreases with an increase in Λ, whereas it increases with an increase in $\chi\Theta$. The partition of the generated heat occurs due to the ratio of $K_1/\sqrt{k_1\tau_1}$ and $K_2/\sqrt{k_2\tau_2}$. These results agree with those obtained by Nosko [23].

Bring into consideration the 'mixed' heat conduction when one of the semispaces conducts heat due to the Fourier heat flux law of Eq.(1), whilst the other one conducts heat due to the Cattaneo heat flux law of Eq.(3), i.e. it holds that $\alpha_1 = 1$ and $\alpha_2 = 0$ or, inversely, $\alpha_1 = 0$ and $\alpha_2 = 1$. As yields from Eq.(34), under the mixed heat conduction, the total generated heat passes to

the Fourier heat conduction semispace at the initial time. Thereby, a Cattaneo heat conduction material coupled with a Fourier heat conduction material exhibits perfect insulating property for ultrashort interfacial heating.

Now it is turn to consider the case of large time variable η. The limit expressions of Eq.(23) and Eq.(24) at real-valued $s \to 0$ take the form

$$\tilde{\vartheta}_{\mathrm{c}} \cong \frac{\sqrt{\chi}}{(\Lambda+\sqrt{\chi})s\sqrt{s}};$$
$$\tilde{Q}_{\mathrm{c1}} \cong \frac{\sqrt{\chi}}{(\Lambda+\sqrt{\chi})s}$$

which correspond to the limit expressions of the corresponding original functions at $\eta \to \infty$ as follows:

$$\vartheta_{\mathrm{c}} \cong \frac{2\sqrt{\chi}}{\sqrt{\pi}(\Lambda+\sqrt{\chi})}\sqrt{\eta};$$
$$Q_{\mathrm{c1}} \cong \frac{\sqrt{\chi}}{\Lambda+\sqrt{\chi}} \tag{35}$$

The dimensional form of Eq.(35) reads

$$T_{\mathrm{c}} \cong \frac{2q_0\sqrt{t}}{\sqrt{\pi}\left(K_1/\sqrt{k_1}+K_2/\sqrt{k_2}\right)};$$
$$q_{\mathrm{c1}} \cong \frac{K_1/\sqrt{k_1}}{K_1/\sqrt{k_1}+K_2/\sqrt{k_2}}\,q_0 \tag{36}$$

The asymptotic expressions of Eq.(36) suggest that the influence of the parameters $\alpha_{1,2}$ and $\tau_{1,2}$ weakens with increasing time variable t, and the behaviour of T_{c} and $q_{\mathrm{c1},2}$ becomes equivalent to that solely governed by Fourier heat conduction as $t \to \infty$.

Table 1 summarises the expressions of the heat partition coefficient q_{c1}/q_0 given by Eq.(34) and Eq.(36). Note that for $\alpha_1 = \alpha_2 \neq 0$, i.e. for equal relative contributions of Fourier heat conduction in the semispaces, the initial rise of q_{c1} (at $t \to 0$) coincides with its limit value at $t \to \infty$.

6. Parametric analysis

The expressions of Eq.(26) for the contact temperature ϑ_{c} and Eq.(27) for the contact heat fluxes $Q_{\mathrm{c1},2}$ incorporate the parameters $\alpha_{1,2}$, Λ, χ and Θ. The influence of each of the parameters is analysed in this section for different types of heat conduction. For simplicity, the specific power is assumed to be constant and equal to $Q_{\mathrm{s}} = 1$.

Fig.5 illustrates the influence of the thermal conductivity ratio $\Lambda = K_2/K_1$. It is seen that both ϑ_c and Q_{c1} decrease with an increase in Λ. This result is explained by the fact that an increase in Λ implies an increase in K_2, i.e. an increased ability of the semispace 2 to remove heat from the contact region. Jeffreys heat conduction (e.g. $\alpha_1 = \alpha_2 = 1/2$) leads to ϑ_c which is above the value for Fourier heat conduction ($\alpha_1 = \alpha_2 = 1$) and below the value for Cattaneo heat conduction ($\alpha_1 = \alpha_2 = 0$). With increasing η, regardless of the heat conduction type, ϑ_c tends to the asymptotic expression of Eq.(35) that corresponds to Fourier heat conduction.

Fig.6 shows the influence of the thermal diffusivity ratio $\chi = k_2/k_1$. An increase in χ, i.e. an increase in k_2, leads to the thermal process intensification in the semispace 2 which is accompanied by an increase in both ϑ_c and Q_{c1}. It is remarkable that in Fig.5 and Fig.6, Q_{c1} (and, accordingly, Q_{c2}) is constant with time, which is due to equal relative contributions of Fourier heat conduction in the semispaces at $\alpha_1 = \alpha_2$ and equal thermal relaxation times $\tau_{1,2}$ at $\Theta = 1$.

Further, Fig.7 presents the influence of the thermal relaxation time ratio $\Theta = \tau_2/\tau_1$. As $\Theta \neq 1$, i.e. $\tau_1 \neq \tau_2$, the character of Q_{c1} (and, accordingly, Q_{c2}) becomes variable. An increase in Θ, i.e. an increase in τ_2, yields an increase in both ϑ_c and Q_{c1}. This looks natural since the increase in τ_2 implies a slower thermal wave propagation in the semispace 2 and, therefore, a less intensive heat removal from the contact region. With increasing η, Q_{c1} tends to its limit value of Eq.(35) which is independent of Θ and $\alpha_{1,2}$.

Finally, Fig.8 shows the sensitivity of the behaviour of ϑ_c and Q_{c1} to variation of the coefficients $\alpha_{1,2}$. The curves of ϑ_c corresponding to Jeffreys heat conduction (e.g. $\alpha_1 = \alpha_2 = 1/2$) and the mixed heat conduction ($\alpha_1 = 1$ and $\alpha_2 = 0$ or, inversely, $\alpha_1 = 0$ and $\alpha_2 = 1$) lie above the curve for Fourier heat conduction and below that for Cattaneo heat conduction. As regards Q_{c1}, under the mixed heat conduction, the initial rise of Q_{c1} equals unit at $\alpha_1 = 1$ and $\alpha_2 = 0$, whereas it equals zero in the opposite case, as $\alpha_1 = 0$ and $\alpha_2 = 1$. This result agrees with those obtained in Section 5 and summarised in Table 1.

Of particular interest is the thermal behaviour under the condition of $\Lambda = \chi = \Theta = 1$ and $\alpha_1 = \alpha_2$. The semispaces exhibit the same thermal properties, which leads to the spatial distributions of $\vartheta_{1,2}$ that are symmetrical with respect to the contact plane $\xi = 0$ for all considered types of heat conduction. The generated heat is partitioned equally between the semispaces, i.e. $Q_{c1} = |Q_{c2}| = 1/2$, as shown in Figs.5–8.

7. Solution application

Apply the obtained solution given by Eq.(26) and Eq.(27) to the simulation problem of ultrashort laser pulse welding. The properties of the welded pieces 1 and 2 are as follows: thermal

conductivities $K_1 = 10$ W/(m °C) and $K_2 = 1$ W/(m °C); thermal diffusivities $k_1 = 10^{-5}$ m^2/s and $k_2 = 10^{-6}$ m^2/s; thermal relaxation times $\tau_1 = 1$ ps and $\tau_2 = 10$ ps. By order of magnitude, the properties of the piece 1 are typical for metals, whilst those of the piece 2 are typical for dielectric materials (Guillemet and Bardon [56]). The initial temperature of the pieces equals $T_0 = 20$ °C. The contact region between the pieces is heated by a laser with variable specific power q_s in the time interval from zero to $t_s = 1$ ps. Two regimes of heating, namely, linear and quadratic, are considered, as illustrated in Fig.9. The linear regime is described by the specific power $q_s = q_0(1 - t/t_s)$, i.e. $n = 1$, $p_0 = 1$ and $p_1 = -t_s^{-1}$ are specified in Eq.(11), which represents a ramp-down pulse shaping used to improve the welding characteristics (Zhang et al. [57]). As regards the quadratic regime, here the specific power is given by the function $q_s = 4q_0\, t/t_s\, (1 - t/t_s)$, i.e. $n = 2$, $p_0 = 0$, $p_1 = 4/t_s$ and $p_2 = -4/t_s^2$ are specified in Eq.(11). This function looks to be a good approximation of a single ultrashort laser pulse (Ullsperger et al. [58]). The maximum value of the specific power q_s is set equal to $q_0 = 10^{12}$ W/m^2 for both regimes.

The linear regime is characterised by a step change of q_s at the initial time (see Fig.9). This step change results in a qualitatively different behaviour of the contact temperature T_c depending on the heat conduction type, as shown in Fig.10. Under Fourier heat conduction, the maximum value of T_c is 148 °C at exactly 0.5 ps. Under Jeffreys heat conduction at $\alpha_1 = \alpha_2 = 1/2$, T_c reaches its maximum of 181°C at 0.43 ps. Cattaneo heat conduction results in a step increase in T_c to the value of 307 °C at the initial time and subsequent decrease in T_c. A qualitatively different behaviour can be also noticed for the contact heat flux q_{c1} under the mixed heat conduction at $\alpha_1 = 0$ and $\alpha_2 = 1$.

In contrast to the linear regime considered above, the quadratic regime provides continuous and symmetric variation of q_s (see Fig.9). The behaviour of T_c and q_{c1} is not affected qualitatively by the heat conduction type. Both relative contact temperature $(T_c - T_0)$ and q_{c1} start increasing from zero at the initial time, as shown in Fig.11. There is, however, a significant difference in the maximum value of T_c. It varies from 208 °C at 0.74 ps for Fourier heat conduction to 352 °C at 0.55 ps for Cattaneo heat conduction.

It is noteworthy that under Fourier heat conduction, the contact heat flux q_{c1} obeys the following equation (Carslaw and Jaeger [53]):

$$q_{c1} = \frac{K_1/\sqrt{k_1}}{K_1/\sqrt{k_1} + K_2/\sqrt{k_2}}\, q_s$$

Accordingly, q_{c1} turns zero at the final time $t = t_s$ for both regimes. On the other hand, under Jeffreys heat conduction or its non-Fourier particular case, q_{c1} takes a non-zero value at the final time (see Fig.10 and Fig.11), which suggests a residual heat transfer through the contact region.

As mentioned in Section 1, for geometrically one-dimensional space, Jeffreys heat conduction due to Eq.(6) is equivalent to the Guyer-Krumhansl equation as the dissipation parameter $l^2 = \alpha\tau k$. This implies that the temperature solutions based on Eq.(6) can be potentially applied to investigating the Guyer-Krumhansl heat conduction problems by adjusting the coefficient α which is not bounded above by unit anymore. For example, Fig.10 and Fig.11 show the curves 'Guyer-Krumhansl' determined by Eq.(26) and Eq.(27) at $\alpha_1 = \alpha_2 = 2$. It is seen that the Guyer-Krumhansl curve T_c lies noticeably lower compared to that for Fourier heat conduction, whilst the difference in the respective curves of $q_{\mathrm{c}1}$ is small. Note that the presented Guyer-Krumhansl curves correspond to the contact conditions of Eqs.(10)–(12) based on the Jeffreys heat flux law of Eq.(5) and, therefore, do not simulate pure Guyer-Krumhansl heat conduction. A more detailed analysis of the relationship between the Jeffreys and Guyer-Krumhansl types of heat conduction may be the subject of further studies.

Thereby, the simulations above illustrate the applicability of the solution given by Eq.(26) and Eq.(27). The obtained results highlight the importance of choosing the adequate type of heat conduction.

8. Conclusions

The problem of Jeffreys heat conduction in coupled semispaces subjected to the action of an interfacial heat source was defined. The analytical expressions of the contact temperature T_c and heat fluxes $q_{\mathrm{c}1,2}$ were derived in the dimensionless form of Eq.(26) and Eq.(27) for a polynomial specific power of the heat source using the Laplace transform approach. They were validated by comparisons to the known analytical expressions and numerically calculated values. The asymptotic behaviour of the contact temperature T_c and heat flux $q_{\mathrm{c}1}$ was analysed for Jeffreys, Cattaneo, Fourier and mixed types of heat conduction. The parametric analysis was performed for different ratios of thermal conductivities $K_{1,2}$, thermal diffusivities $k_{1,2}$, thermal relaxation times $\tau_{1,2}$ and coefficients $\alpha_{1,2}$ indicating the relative contribution of Fourier heat conduction. The solution was shown to be applicable on the simulation example of ultrashort laser pulse welding. The key findings can be formulated as follows:

- Jeffreys heat conduction results in continuous variation of the contact temperature T_c, whilst its particular case — Cattaneo heat conduction — is accompanied by a step change of T_c at the initial time, as described by Eq.(33).
- The initial heat partition occurs due to the ratio of $K_1\sqrt{\alpha_1/k_1}$ and $K_2\sqrt{\alpha_2/k_2}$ under Jeffreys heat conduction and due to the different ratio of $K_1/\sqrt{k_1\tau_1}$ and $K_2/\sqrt{k_2\tau_2}$ under Cattaneo heat conduction, as described by Eq.(34).

- Under the contact of a Fourier heat conduction material and a Cattaneo heat conduction material, the total generated heat passes to the Fourier heat conduction material at the initial time.
- The influence of the heat conduction type on the contact temperature T_c and heat fluxes $q_{c1,2}$ is crucial in the start interval of time. The behaviour of T_c and $q_{c1,2}$ tends to that solely governed by Fourier heat conduction with time.

Acknowledgement

Computations were carried out at the Centre of Informatics Tricity Academic Supercomputer & Network (Poland).

This research did not receive any specific grant from funding agencies in the public, commercial, or not-for-profit sectors.

References

[1] J. Fourier, Théorie analytique de la chaleur, F. Didot, Paris, 1822.

[2] H.S. Carslaw, Introduction to the mathematical theory of the conduction of heat in solids, 2nd ed., Macmillan and Co., London, 1921.

[3] W.A. Mersman, Heat conduction in an infinite composite solid with an interface resistance, Transactions of the American Mathematical Society 53 (1) (1943) 14–24.

[4] S.A. Schaaf, On the superposition of a heat source and contact resistance, Quarterly of Applied Mathematics 5 (1) (1947) 107–111.

[5] V. Peshkov, Second sound in helium II, Journal of Physics 8 (1944) 381–389.

[6] C.C. Ackerman, B. Bertman, H.A. Fairbank, R.A. Guyer, Second sound in solid helium, Physical Review Letters 16 (18) (1966) 789–791.

[7] J.C. Maxwell, On the dynamical theory of gases, Philosophical Transactions of the Royal Society of London 157 (1867) 49–88.

[8] L. Landau, The theory of superfluidity of helium II, Physical Review 60 (1941) 356–358.

[9] C. Cattaneo, Sur une forme de l'équation de la chaleur éliminant le paradoxe d'une propagation instantanée, Comptes rendus hebdomadaires des séances de l'Académie des Sciences 247 (1958) 431–433.

[10] P. Vernotte, Les paradoxes de la théorie continue de l'équation de la chaleur, Comptes rendus hebdomadaires des séances de l'Académie des Sciences 246 (1958) 3154–3155.

[11] D.D. Joseph, L. Preziosi, Heat waves, Reviews of Modern Physics 61 (1) (1989) 41–73.

[12] M.S. Kazimi, C.A. Erdman, On the interface temperature of two suddenly contacting materials, Journal of Heat Transfer 97 (4) (1975) 615–617.

[13] J.I. Frankel, B. Vick, M.N. Özisik, General formulation and analysis of hyperbolic heat conduction in composite media, International Journal of Heat and Mass Transfer 30 (7) (1987) 1293–1305.

[14] D.Y. Tzou, Reflection and refraction of thermal waves from a surface or an interface between dissimilar materials, International Journal of Heat and Mass Transfer 36 (2) (1993) 401–410.

[15] W.B. Lor, H.S. Chu, Hyperbolic heat conduction in thin-film high T_c superconductors with interface thermal resistance, Cryogenics 39 (1999) 739–750.

[16] W.B. Lor, H.S. Chu, Effect of interface thermal resistance on heat transfer in a composite medium using the thermal wave model, International Journal of Heat and Mass Transfer 43 (2000) 653–663.

[17] P. Duhamel, A new finite integral transform pair for hyperbolic conduction problems in heterogeneous media, International Journal of Heat and Mass Transfer 44 (2001) 3307–3320.

[18] A.F. Khadrawi, M.A. Al-Nimr, M. Hammad, Thermal behavior of perfect and imperfect contact composite slabs under the effect of the hyperbolic heat conduction model, International Journal of Thermophysics 23 (2) (2002) 581–598.

[19] C.S. Tsai, C.I. Hung, Thermal wave propagation in a bi-layered composite sphere due to a sudden temperature change on the outer surface, International Journal of Heat and Mass Transfer 46 (2003) 5137–5144.

[20] W. Dai, T. Niu, A finite difference scheme for solving a nonlinear hyperbolic two-step model in a double-layered thin film exposed to ultrashort-pulsed lasers with nonlinear interfacial conditions, Nonlinear Analysis: Hybrid Systems 2 (2008) 121–143.

[21] T. Niu, W. Dai, A hyperbolic two-step model based finite difference scheme for studying thermal deformation in a double-layered thin film exposed to ultrashort-pulsed lasers, International Journal of Thermal Sciences 48 (2009) 34–49.

[22] J. Ordóñez-Miranda, J.J. Alvarado-Gil, Thermal wave oscillations and thermal relaxation time determination in a hyperbolic heat transport model, International Journal of Thermal Sciences 48 (2009) 2053–2062.

[23] O. Nosko, Perfect thermal contact of hyperbolic conduction semispaces with an interfacial heat source, International Journal of Heat and Mass Transfer 164 (2021) 120541.

[24] C.C. Ackerman, R.A. Guyer, Temperature pulses in dielectric solids, Annals of Physics 50 (1) (1968) 128–185.

[25] T.F. McNelly, S.J. Rogers, D.J. Channin, R.J. Rollefson, W.M. Goubau, G.E. Schmidt, J.A. Krurnhansl, R.O. Pohl, Heat pulses in NaF: Onset of second sound, Physical Review Letters 24 (3) (1970) 100–102.

[26] J. Li, Y. Gu, Z. Guo, Analysis of the phenomena of non-Fourier heat conduction in switch-Q laser processing for reducing the core loss of grain-oriented silicon steel, Journal of Materials Processing Technology 74 (1998) 292–297.

[27] F. Jiang, Non-Fourier heat conduction phenomena in porous material heated by microsecond laser pulse, Microscale Thermophysical Engineering 6 (4) (2003) 331–346.

[28] A. Banerjee, A.A. Ogale, C. Das, K. Mitra, C. Subramanian, Temperature distribution in different materials due to short pulse laser irradiation, Heat Transfer Engineering 26 (8) (2005) 41–49.

[29] K.K. Tamma, X. Zhou, Macroscale and microscale thermal transport and thermo-mechanical interactions: some noteworthy perspectives, Journal of Thermal Stresses 21 (3–4) (1998) 405–449.

[30] R.A. Guyer, J.A. Krumhansl, Solution of the linearized phonon Boltzmann equation, Physical Review 148 (2) (1966) 778–788.

[31] A. Fehér, R. Kovács, On the evaluation of non-Fourier effects in heat pulse experiments, International Journal of Engineering Science 169 (2021) 103577.

[32] A.J.A. Ramos, R. Kovács, M.M. Freitas, D.S. Almeida Júnior, Mathematical analysis and numerical simulation of the Guyer–Krumhansl heat equation, Applied Mathematical Modelling 115 (2023) 191–202.

[33] S. Both, B. Czél, T. Fülöp, Gy. Gróf, Á. Gyenis, R. Kovács, P. Ván, J. Verhás, Deviation from the Fourier law in room-temperature heat pulse experiments, Journal of Non-Equilibrium Thermodynamics 41 (1) (2016) 41–48.

[34] P. Ván, A. Berezovski, T. Fülöp, Gy. Gróf, R. Kovács, Á. Lovas, J. Verhás, Guyer-Krumhansl-type heat conduction at room temperature, Europhysics Letters 118 (5) (2017) 50005.

[35] D.Y. Tzou, The generalized lagging response in small-scale and high-rate heating, International Journal of Heat and Mass Transfer 38 (17) (1995) 3231–3240.

[36] M. Fabrizio, B. Lazzari, Stability and Second Law of Thermodynamics in dual-phase-lag heat conduction, International Journal of Heat and Mass Transfer 74 (2014) 484–489.

[37] S.A. Rukolaine, Unphysical effects of the dual-phase-lag model of heat conduction, International Journal of Heat and Mass Transfer 78 (2014) 58–63.

[38] E. Awad, Dual-phase-lag in the balance: Sufficiency bounds for the class of Jeffreys' equations to furnish physical solutions, International Journal of Heat and Mass Transfer 158 (2020) 119742.

[39] J.R. Ho, C.P. Kuo, W.S. Jiaung, Study of heat transfer in multilayered structure within the framework of dual-phase-lag heat conduction model using lattice Boltzmann method, International Journal of Heat and Mass Transfer 46 (2003) 55–69.

[40] M.A. Al-Nimr, M. Naji, R.I. Abdallah, Thermal behavior of a multi-layered thin slab carrying periodic signals under the effect of the dual-phase-lag heat conduction model, International Journal of Thermophysics 25 (3) (2004) 949–966.

[41] N.S. Al-Huniti, M.A. Al-Nimr, Thermoelastic behavior of a composite slab under a rapid dual-phase-lag heating, Journal of Thermal Stresses 27 (7) (2004) 607–623.

[42] Y.M. Lee, T.W. Tsai, Ultra-fast pulse-laser heating on a two-layered semi-infinite material with interfacial contact conductance, International Communications in Heat and Mass Transfer 34 (2007) 45–51.

[43] K. Ramadan, Semi-analytical solutions for the dual phase lag heat conduction in multilayered media, International Journal of Thermal Sciences 48 (2009) 14–25.

[44] K. Ramadan, M.A. Al-Nimr, Analysis of the thermal behavior of a multilayer slab with imperfect contact using the dual-phase-lag heat conduction model, Journal of Heat Transfer 130 (2008) 074501.

[45] A.H. Akbarzadeh, D. Pasini, Phase-lag heat conduction in multilayered cellular media with imperfect bonds, International Journal of Heat and Mass Transfer 75 (2014) 656–667.

[46] G.H. Yeoh, X. Gu, V. Timchenko, S.M. Valenzuela, B.A. Cornell, High order accurate dual-phase-lag numerical model for microscopic heating in multiple domains, International Communications in Heat and Mass Transfer 78 (2016) 21–28.

[47] T. Xue, X. Zhang, K.K. Tamma, Investigation of thermal inter-facial problems involving non-locality in space and time, International Communications in Heat and Mass Transfer 99 (2018) 37–42.

[48] T. Xue, X. Zhang, K.K. Tamma, On a generalized non-local two-temperature heat transfer DAE modeling/simulation methodology for metal-nonmetal thermal inter-facial problems, International Journal of Heat and Mass Transfer 138 (2019) 508–515.

[49] J. Ma, Y. Sun, J. Yang, Analytical solution of dual-phase-lag heat conduction in a finite medium subjected to a moving heat source, International Journal of Thermal Sciences 125 (2018) 34–43.

[50] F. Xu, K.A. Seffen, T.J. Lu, Non-Fourier analysis of skin biothermomechanics, International Journal of Heat and Mass Transfer 51 (2008) 2237–2259.

[51] O. Nosko, Hyperbolic heat conduction at a microscopic sliding contact with account of adhesion-deformational heat generation and wear, International Journal of Thermal Sciences 137 (2019) 101−109.

[52] G. Doetsch, Introduction to the theory and application of the Laplace transformation, Springer, Berlin, 1974.

[53] H.S. Carslaw, J.C. Jaeger, Conduction of heat in solids, 2nd ed., Oxford University Press, London, 1959.

[54] E. Awad, T. Sandev, R. Metzler, A. Chechkin, From continuous-time random walks to the fractional Jeffreys equation: Solution and properties, International Journal of Heat and Mass Transfer 181 (2021) 121839.

[55] M.N. Özişik, D.Y. Tzou, On the wave theory in heat conduction, Journal of Heat Transfer 116 (3) (1994) 526–535.

[56] P. Guillemet, J.P. Bardon, Conduction de la chaleur aux temps courts: les limites spatio-temporelles des modèles parabolique et hyperbolique, International Journal of Thermal Sciences 39 (2000) 968–982.

[57] P. Zhang, Z. Jia, Z. Yu, H. Shi, S. Li, D. Wu, H. Yan, X. Ye, J. Chen, F. Wang, Y. Tian, A review on the effect of laser pulse shaping on the microstructure and hot cracking behavior in the welding of alloys, Optics and Laser Technology 140 (2021) 107094.

[58] T. Ullsperger, D. Liu, B. Yürekli, G. Matthäus, L. Schade, B. Seyfarth, H. Kohl, R. Ramm, M. Rettenmayr, S. Nolte, Ultra-short pulsed laser powder bed fusion of Al-Si alloys: Impact of pulse duration and energy in comparison to continuous wave excitation, Additive Manufacturing 46 (2021) 102085.

Table 1. Asymptotic expressions of the heat partition coefficient q_{c1}/q_0

Heat conduction type	Asymptotic at $t \to 0$	Asymptotic at $t \to \infty$
Fourier at $\alpha_1 = \alpha_2 = 1$	$\frac{K_1/\sqrt{k_1}}{K_1/\sqrt{k_1} + K_2/\sqrt{k_2}}$	$\frac{K_1/\sqrt{k_1}}{K_1/\sqrt{k_1} + K_2/\sqrt{k_2}}$
Jeffreys at $\alpha_1 \neq 0$ or $\alpha_2 \neq 0$	$\frac{K_1\sqrt{\alpha_1/k_1}}{K_1\sqrt{\alpha_1/k_1} + K_2\sqrt{\alpha_2/k_2}}$	
Jeffreys at $\alpha_1 = \alpha_2 \neq 0$	$\frac{K_1/\sqrt{k_1}}{K_1/\sqrt{k_1} + K_2/\sqrt{k_2}}$	
Cattaneo at $\alpha_1 = \alpha_2 = 0$	$\frac{K_1/\sqrt{k_1\tau_1}}{K_1/\sqrt{k_1\tau_1} + K_2/\sqrt{k_2\tau_2}}$	
Mixed at $\alpha_1 = 1$ and $\alpha_2 = 0$	1	
Mixed at $\alpha_1 = 0$ and $\alpha_2 = 1$	0	

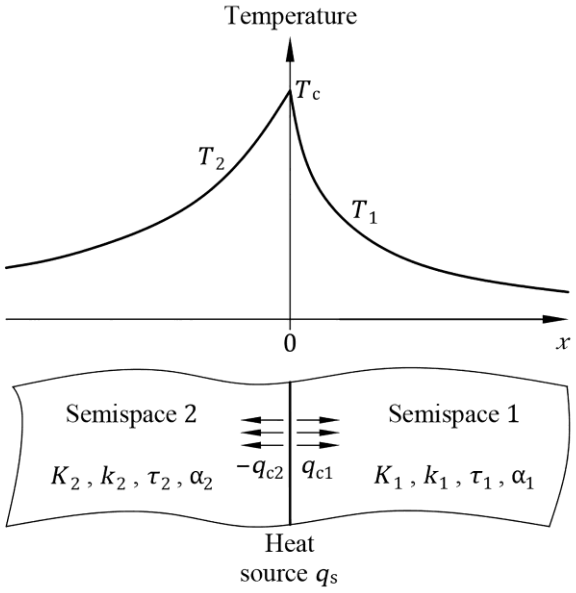

Fig.1. Schematic of the contact heat conduction problem

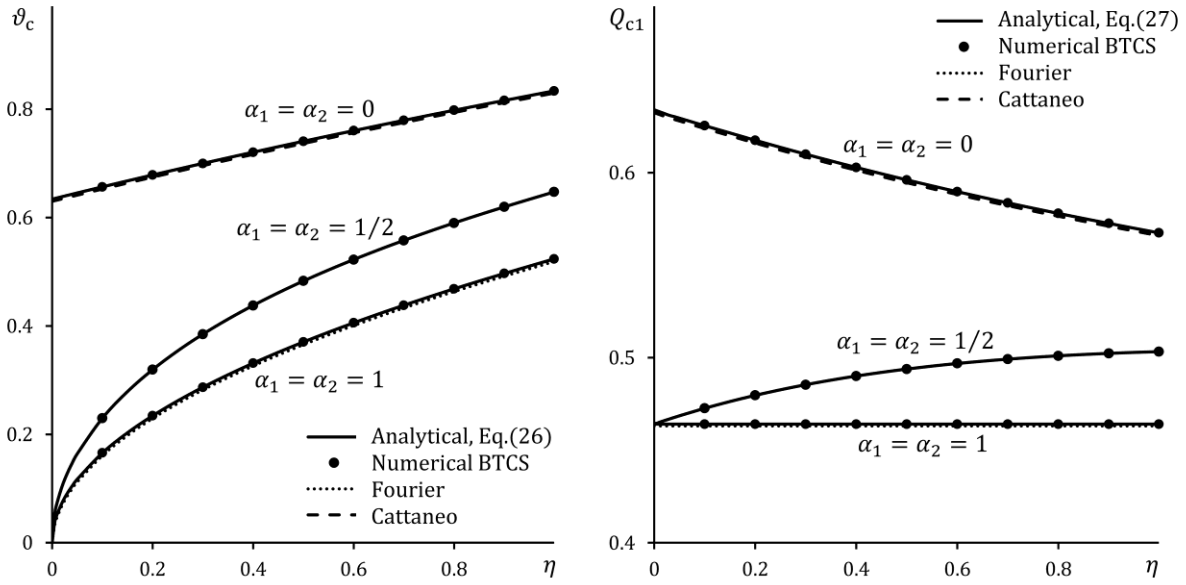

Fig.2. Validation of the analytical solution of Eq.(26) and Eq.(27) at $Q_s = 1$, $\Lambda = 2$, $\chi = 3$, $\Theta = 4$

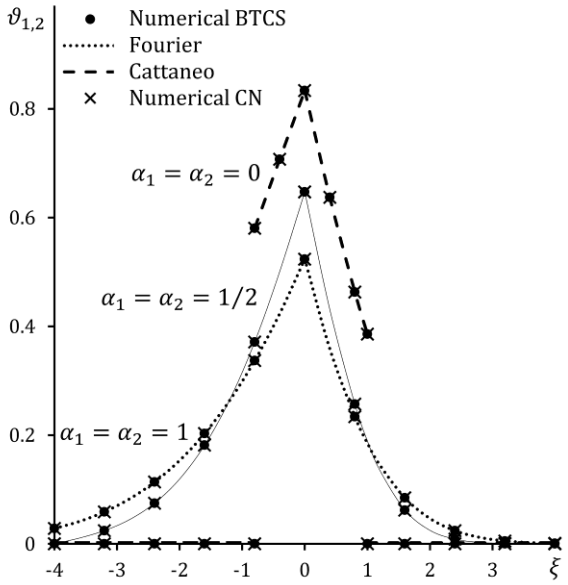

Fig.3. Validation of the numerical algorithm at $Q_s = 1$, $\Lambda = 2$, $\chi = 3$, $\Theta = 4$, $\eta = 1$

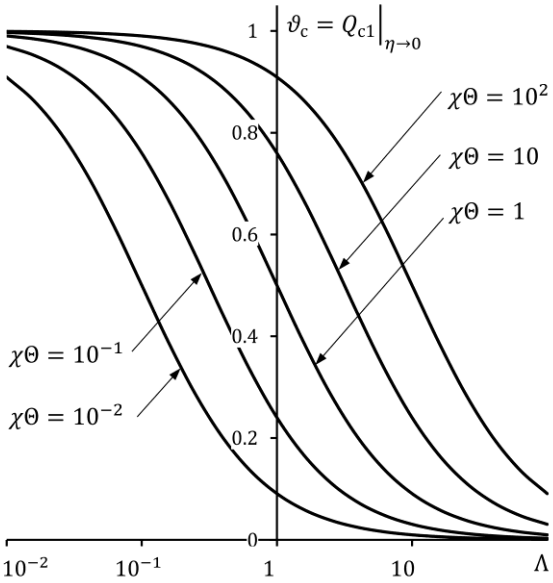

Fig.4. Initial rise of the contact temperature ϑ_c under Cattaneo heat conduction at $\alpha_1 = \alpha_2 = 0$ and $Q_s = 1$

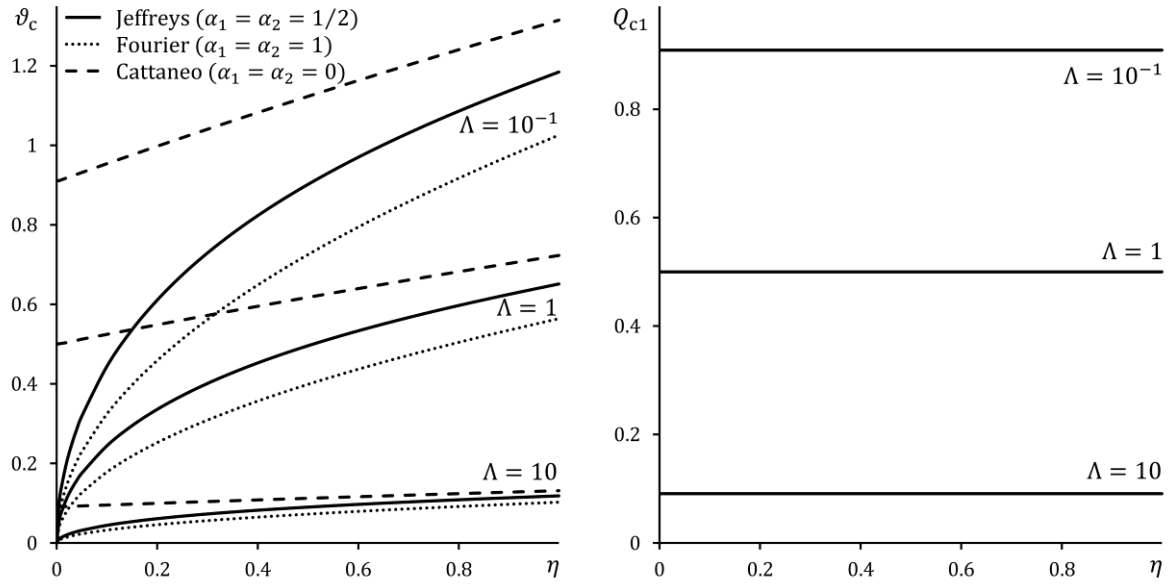

Fig.5. Influence of the thermal conductivity ratio Λ on the contact temperature ϑ_c and heat flux Q_{c1} at $\chi = \Theta = 1$ and $Q_s = 1$

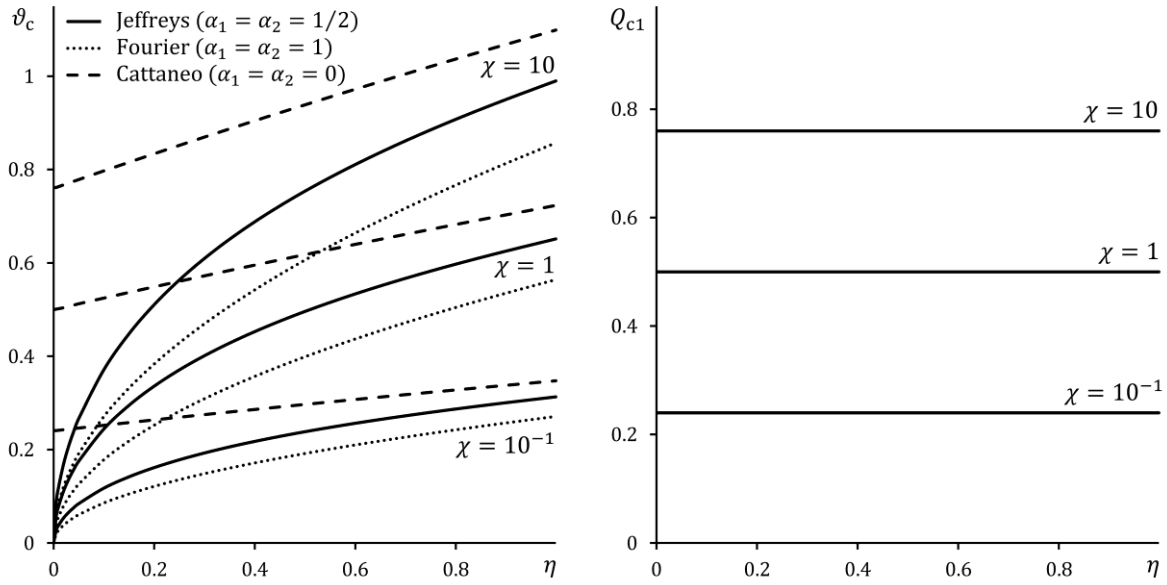

Fig.6. Influence of the thermal diffusivity ratio χ on the contact temperature ϑ_c and heat flux Q_{c1} at $\Lambda = \Theta = 1$ and $Q_s = 1$

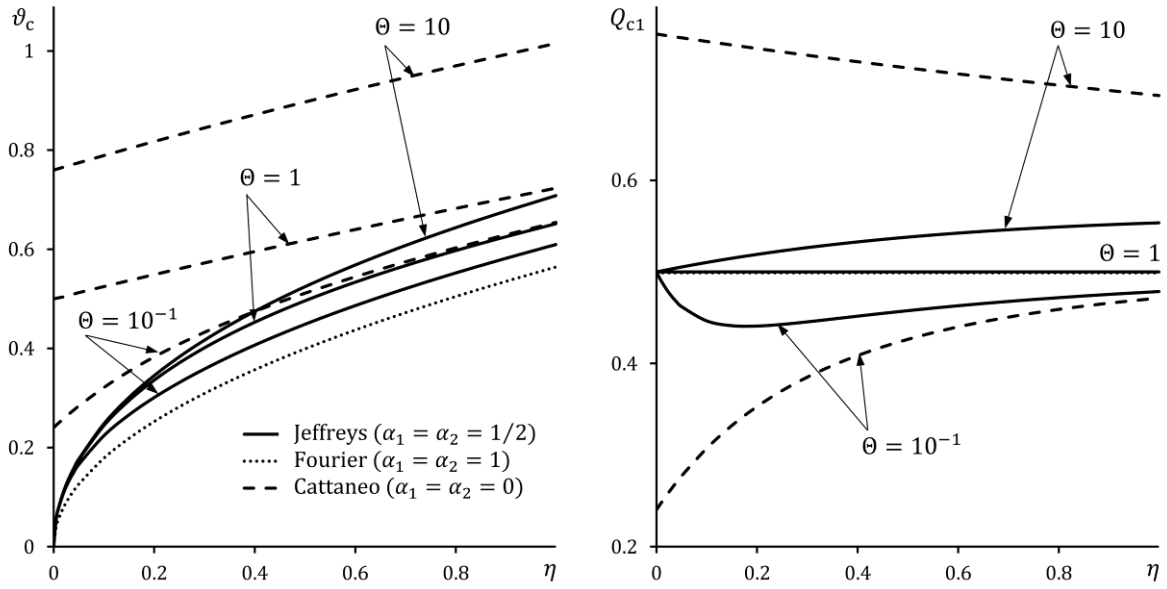

Fig.7. Influence of the thermal relaxation time ratio Θ on the contact temperature ϑ_c and heat flux Q_{c1} at $\Lambda = \chi = 1$ and $Q_s = 1$

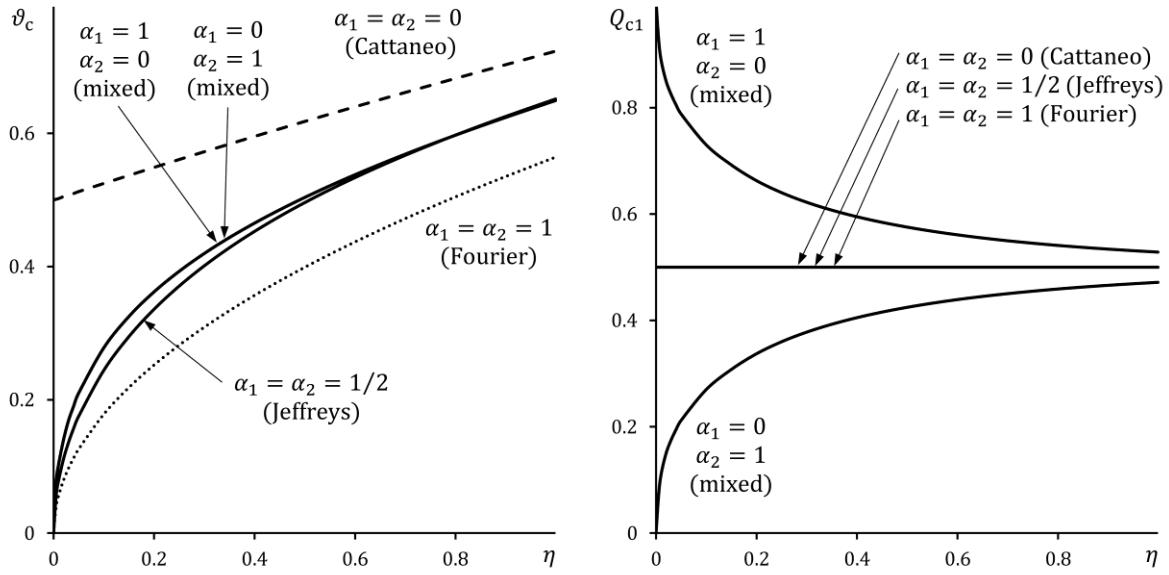

Fig.8. Influence of the coefficients $\alpha_{1,2}$ on the contact temperature ϑ_c and heat flux Q_{c1} at $\Lambda = \chi = \Theta = 1$ and $Q_s = 1$

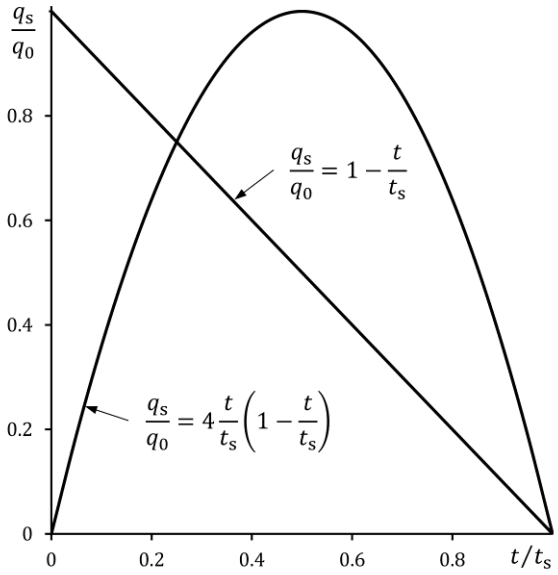

Fig.9. Time dependency of the specific power q_s

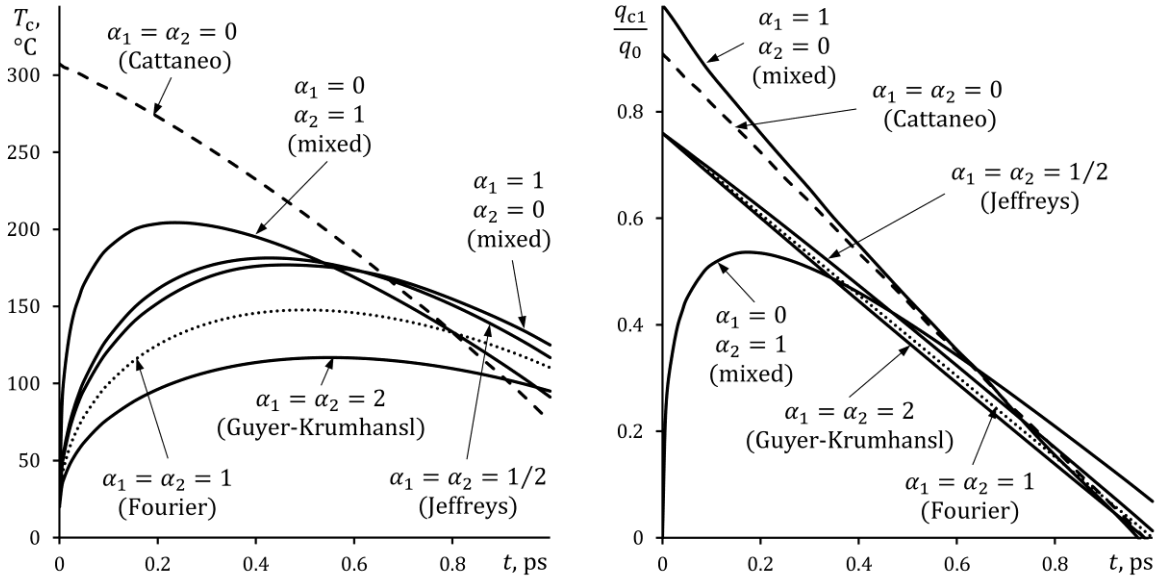

Fig.10. Contact temperature T_c and heat flux q_{c1} under different types of heat conduction and linear specific power $q_s = q_0(1 - t/t_s)$

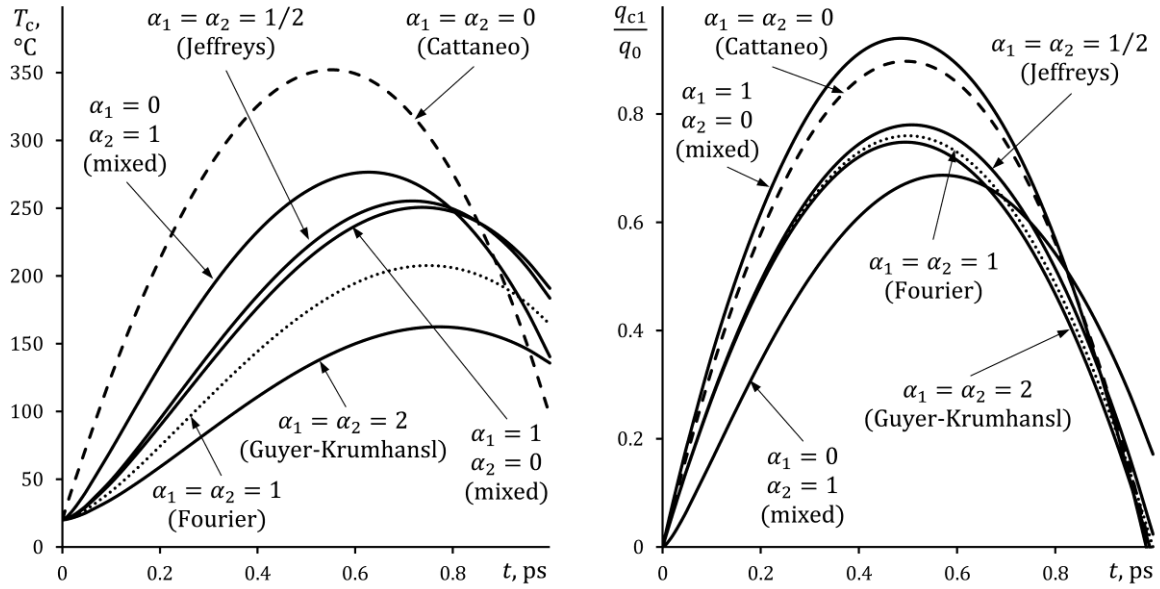

Fig.11. Contact temperature T_c and heat flux q_{c1} under different types of heat conduction and quadratic specific power $q_s = 4q_0\, t/t_s\,(1 - t/t_s)$